

Constraining the maximum depth of brittle deformation at slow- and ultraslow-spreading ridges using microseismicity

Vera Schlindwein*

Alfred Wegener Institute Helmholtz Centre for Polar and Marine Research, Am Alten Hafen 26, D 27568 Bremerhaven, Germany
*E-mail: Vera.Schlindwein@awi.de

The different earthquake location results in Schlindwein and Schmid (2016) and Grevemeyer et al. (2019) for the SWEAP (Southwest Indian Ridge Earthquakes and Plumes) region demonstrate the difficulties inherent in this particular passive seismological data set. Large travel time residuals in the initial location require a careful choice of the location approach and a thorough assessment of the location results. The root-mean-square residual (rms) should not be used as sole criterion to judge the location quality (e.g., Husen and Smith, 2004). Here, I reevaluate the location quality using the same algorithm as Grevemeyer et al., but in contrast to their approach I select a solution based on multiple criteria. I restrict this test to the 202 best recorded events that have an azimuth gap $<180^\circ$ and are detected by all 8 stations with at least 3 S-phases at stations unaffected by soft sediments. For an initial location run, I exclude S-phases of stations SWE05, 06, 08 and 09 that suffer from large delays to avoid a bias of the initial location. Average station residuals, excluding individual residuals larger than 3 s, serve as station correction terms for P- and S-phases, respectively. Subsequent inversion runs use all available phases, since S-phases were prominently visible in the seismograms, and station correction terms are updated after each iteration. The average rms of the earthquakes decreases (Fig. 1a), but location quality as expressed by the spatial distance between the maximum likelihood hypocenter and the expectation hypocenter (termed hypocenter spread hereafter) and the average length of the axes of confidence ellipsoid (termed error ellipse hereafter) deteriorates during inversion. In addition, the station correction terms shift in such a way that the observed S-P travel time difference at all stations shortens, also at stations that are not underlain by soft sediments. As a result, location depths become shallower indicating some trade-off between station corrections and hypocenter depth (Fig. 1b). Using P-phases only yields a low rms associated with low values of the spatial error indicators, but the lack of constraining S-phases produces large error ellipses.

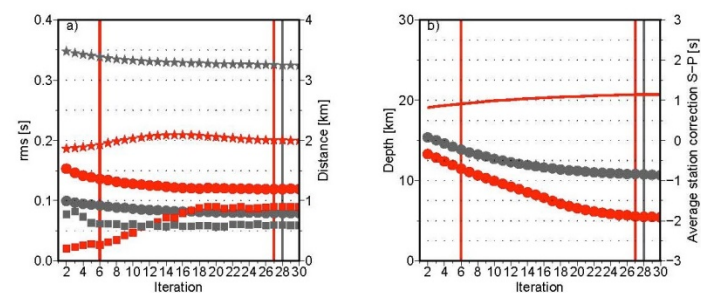


Figure 1. Results of iterative location runs using P- and S-phases (red) and P-phases only (gray). Poorly located events ($\text{rms} > 0.5$ s) are excluded. Vertical lines mark preferred solution (iteration 6), lowest rms solution (iteration 27) and the P-phase only solution (gray, iteration 28). (a) circles: average rms; stars: size of error ellipse (km), squares: hypocenter spread (km). (b) circles: average hypocenter depth below seafloor (km) and average S-P difference of station correction terms (s).

I prefer a compromise solution with an acceptably low rms, low spatial errors, and small station correction terms (iteration 6) over the lowest rms solution (iteration 27) or a solution using P-phases only. Figure 2 shows the probabilistic location uncertainty as density scatter clouds. The hypocenter spread is small in iteration 6 providing a confined band of seismicity depth with a narrow scatter cloud (Fig. 2a). The lowest rms solution

(Fig. 2b), however, shows extended scatter clouds and hypocenter spread especially for events in the west and for shallow events. The P-phase only inversion (Fig. 2c) yields similar results to iteration 6, but uncertainty is much larger due to lacking S-phases. Applying the quality criteria of Husen and Smith (2004) to select very good locations ($\text{rms} < 0.5$ s, hypocenter spread < 0.5 km, error ellipse < 2 km) and good locations ($\text{rms} < 0.5$ s, hypocenter spread < 0.5 km, error ellipse > 2 km) results in 123 very good and 45 good events for the preferred solution, compared to 70 very good and 29 good events for the minimum rms solution and only 153 good events for the P-phase solution, clearly indicating solid results for iteration 6.

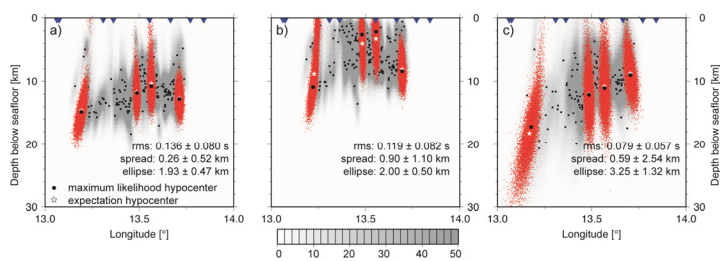


Figure 2. Location results with combined scatter density clouds (gray) showing overall location uncertainty and average location quality indicators. Scatter samples of four example events are highlighted in red. (a) preferred solution (iteration 6); (b) lowest rms solution (iteration 27); (c) P-phase only solution (iteration 28). Blue triangles mark seismic stations.

Based on this reanalysis of location quality, it appears that seismicity is concentrated in a band between 8 and 20 km depth below seafloor in agreement with Grevemeyer et al.'s figure S5c, but not with their preferred solution that uses iteratively updated station terms. The SWEAP region along with oceanic core complexes at the Mid-Atlantic ridge (deMartin et al., 2007; Parnell-Turner et al., 2017) may therefore well represent examples of areas with aseismic deformation of the uppermost lithosphere. Hydration of the prevailing ultramafic rocks constitutes one effective mechanism to reduce rock strength in these settings (Escartín et al., 2001).

REFERENCES CITED

deMartin, B.J., Sohn, R.A., Pablo Canales, J., and Humphris, S.E., 2007, Kinematics and geometry of active detachment faulting beneath the Trans-Atlantic Geotraverse (TAG) hydrothermal field on the Mid-Atlantic Ridge: *Geology*, v. 35, p. 711–714, <https://doi.org/10.1130/G23718A.1>.
Escartín, J., Hirth, G., and Evans, B., 2001, Strength of slightly serpentinized peridotites: Implications for the tectonics of oceanic lithosphere: *Geology*, v. 29, p. 1023–1026, [https://doi.org/10.1130/0091-7613\(2001\)029<1023:SOSSPI>2.0.CO;2](https://doi.org/10.1130/0091-7613(2001)029<1023:SOSSPI>2.0.CO;2).
Grevemeyer, I., Hayman, N.H., Lange, D., Peirce, C., Papenberg, C., Van Avendonk, H.J.A., Schmid, F., Gómez de La Peña, L., and Dannowski, A., 2019, Constraining the maximum depth of brittle deformation at slow- and ultraslow-spreading ridges using microseismicity: *Geology*, v. 47, p. 1069–1073, <https://doi.org/10.1130/G46577.1>.
Husen, S., and Smith, R.B., 2004, Probabilistic Earthquake Relocation in Three-Dimensional Velocity Models for the Yellowstone National Park Region, Wyoming: *Bulletin of the Seismological Society of America*, v. 94, p. 880–896, <https://doi.org/10.1785/0120030170>.
Parnell-Turner, R., Sohn, R.A., Peirce, C., Reston, T.J., MacLeod, C.J., Searle, R.C., and Simão, N.M., 2017, Oceanic detachment faults generate compression in extension: *Geology*, v. 45, p. 923–926, <https://doi.org/10.1130/G39232.1>.
Schlindwein, V., and Schmid, F., 2016, Mid-ocean ridge seismicity reveals extreme types of ocean lithosphere: *Nature*, v. 535, p. 276–279, <https://doi.org/10.1038/nature18277>.